A quasi-solid-sate and self-powered biosupercapacitor based on flexible nanoporous gold electrodes

Xinxin Xiao, EDMOND MAGNER

Publication date

01-01-2018

Published in

Chemical Communications;

Cite this paper: Xinxin Xiao, Edmond Magner; A quasi-solid-sate and self-powered biosupercapacitor based on flexible nanoporous gold electrodes, ***Chem. Commun***. 2018, DOI: 10.1039/C8CC02555J.

A quasi-solid-sate and self-powered biosupercapacitor based on flexible nanoporous gold electrodes

Xinxin Xiao*, Edmond Magner*

Department of Chemical Sciences and Bernal Institute, University of Limerick, Limerick V94 T9PX, Ireland

E-mail: Xinxin.xiao@ul.ie, edmond.magner@ul.ie; Fax: +353 61 213529; Tel: +353 61 234390

Abstract: A quasi-solid-state and flexible biofuel cell using a hydrogel electrolyte preloaded with sugar as a fuel is described. The device can function as a self-powered biosupercapacitor delivering pulses for over 600 cycles, with a power density over 10 times higher than that from the biofuel cell alone.

Enzymatic biofuel cells (EBFCs) utilise enzymes as catalysts to harvest electricity via the electrochemical oxidation of sugars (e.g. glucose) at a bioanode and the reduction of O_2 at a biocathode[1]. The properties of enzymes (e.g. selectivity, biocompatibility, operation at physiological conditions) enable the use of EBFCs as promising power sources in health-related microelectronic devices operating in biological environments[2, 3]. The use of implantable glucose/O_2 EBFCs has been suggested as potential replacements for Li batteries as continuous power-suppliers for medical implants such as cardiac pacemakers[2]. In parallel with implantable EBFCs that are invasive to the body, non-invasive EBFCs are externally located on the skin or eye, with potential applications as power sources to activate low-energy and bio-integrated wearable electronics[4, 5]. Wang et al. developed a tattoo-type lactate/O_2 EBFC which can be seamlessly attached onto the skin of perspiring human subjects[6] and also described textile-EBFCs that can be attached to the skin to generate electricity from lactate in sweat[7]. However, these skin-worn EBFCs can only be used when the subject is perspiring.

Solid-state hydrogel electrolytes can be used to preload sugar as a fuel for skin borne EBFCs[8]. Ogawa et al. prepared a fructose/O_2 EBFC comprised of a polyacrylamide electrolyte containing fructose[8], for use as a built-in power source for an iontophoresis patch. There have been several reports on fructose/O_2 EBFCs utilising hydrogel electrolytes, such as polyacrylamide[9, 10, 11, 12] and poly(2-hydroxy-ethyl methacrylate) and ethylene glycol methacrylate phosphate copolymers[10]. To date, no reports on the development of quasi-solid-state EBFCs based on glucose/O_2 have been described.

In this contribution, we describe the fabrication of a glucose/O_2 EBFC utilising a poly(vinyl alcohol) (PVA) hydrogel film as the

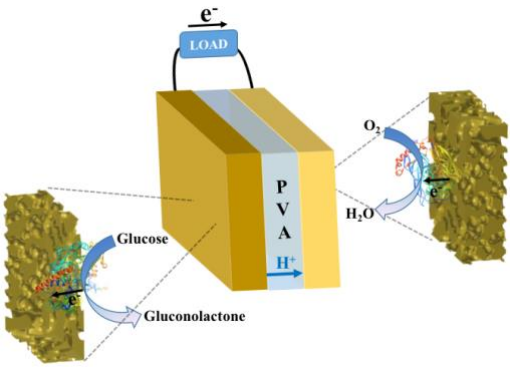

Scheme 1. Setup of the quasi-solid-state biosupercapacitor.

solid-state electrolyte. PVA hydrogels have been widely used for flexible supercapacitors[13, 14] and can be easily prepared by casting aqueous solutions of PVA in a mould. Flexible nanoporous gold (NPG, thickness: 100 nm, pore size: 34.4±4.9 nm, roughness factor: 7.9±1.1, **Fig. 1A**) electrodes were prepared by electrochemically dealloying polyethylene terephthalate (PET) supported $Au_{30}Ag_{70}$ alloy films using a recently reported protocol[15]. *Aspergillus niger* glucose oxidase (GOx) and *Myrothecium verrucaria* bilirubin oxidase (BOx) were separately immobilised onto the anode and cathode, respectively, by cross-linking poly(ethylene glycol) diglycidyl ether (PEGDGE) and osmium polymers that served as electron transfer mediators. [Os(4,4'-dimethyl-2,2'-

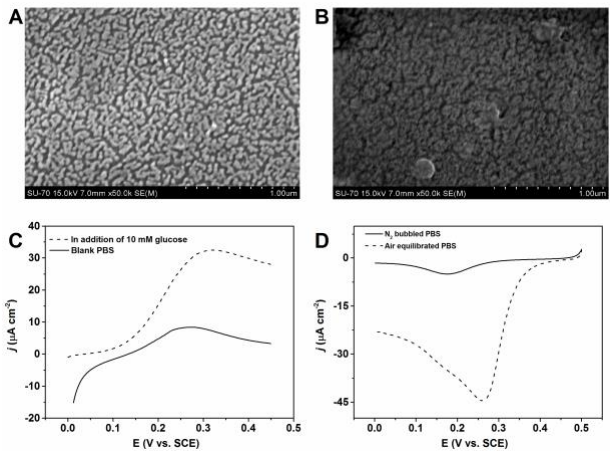

Fig. 1. SEM images of the bare NPG (A) and NPG/Os(dmbpy)$_2$PVI/GOx (B); CVs of the NPG/Os(dmbpy)$_2$PVI/GOx bioanode (C) and NPG/Os(bpy)$_2$PVI/BOx biocathode (D) in 0.1 M pH 7.0 PBS at a scan rate of 5 mV s^{-1}.

bipyridine)$_2$(polyvinylimidazole)$_{10}$Cl]$^{+/2+}$ (Os(dmbpy)$_2$PVI) and [Os(2,2'-bipyridine)$_2$(polyvinylimidazole)$_{10}$Cl]$^{+/2+}$ (Os(bpy)$_2$PVI) were utilised at the bioanode and biocathode, respectively (details in ESI†)[16, 17].

EBFC/supercapacitor hybrids or biosupercapacitors are of interest due to their ability to generate high-power-density pulses [18, 19, 20, 21, 22, 23, 24]. This process relies on self-charging of the capacitive electrodes by the EBFC driven by the potential differences between the bioanode and biocathode [21, 23, 25]. The stored energy generated by the EBFC can then be discharged galvanostatically with high current densities. In comparison to a system that integrates an enzymatic biofuel cell to an external supercapacitor[26], self-powered biosupercapacitors such as the system described here already include the capacitor in comparison to other systems where an external super capacitor is required. The PVA membrane loaded with glucose was sandwiched between the anode and cathode (**Scheme 1**), resulting in a quasi-solid-sate and flexible EBFC that can generate high-power-density pulses for more than 12 hours.

A transparent PVA film (**Fig. S1A**) was obtained by casting a heated (90 °C) solution of 10% PVA in 0.1 M H_3PO_4 into a petri-dish. The film was soaked in 0.1 M KOH to neutralise the solution to a neutral pH, followed by immersion in phosphate buffer solution (PBS) containing 100 mM glucose to store the fuel (details in ESI†). Scanning electron microscope (SEM) images showed that the thickness of the film was ca. 270 µm (**Fig. S2A**). FTIR spectra (**Fig. S2B**) of the dry PVA powder and of the hydrogel possessed a characteristic absorption band at 1082 cm^{-1}, corresponding to a C-O stretching band[27]. Unlike the dry powder, the spectrum of the hydrogel had strong absorption bands at ca. 3300 and 1635 cm^{-1}, due to O-H stretching and bending of water molecules. The water content of the hydrogel, determined using thermogravimetric analysis (TGA) was ca. 57% (**Fig. S2C**). Such a high water-content enables proton conduction between the two electrodes. Using electrochemical impedance spectra (EIS), the ionic conductivity (σ) of the hydrogel film (**Fig. S2D**) was 938 µS cm^{-1}, much higher than that of PVA/H_3PO_4 (22 µS cm^{-1})[28].

Drop-casting of the Os polymer/enzyme mixture blocked the pores of the electrode forming a cap-like modification layer[29] (**Fig. 1B**). Bioelectrodes were characterised separately in three-electrode-cell containing PBS (**Fig. 1C and D**). The NPG/Os(dmbpy)$_2$PVI/GOx bioanode showed a catalytic response (10 mM glucose) with a background-corrected current density (j_{net}, with respect to the geometric area of the electrode) of 25.4±0.6 µA cm^{-2} at +300 mV vs. SCE and an onset potential of ca. 0 mV vs. SCE (**Fig. 1C**). The NPG/Os(bpy)$_2$PVI/BOx biocathode yielded a j_{net} of 25.4±3.3 µA cm^{-2} at +250 mV vs. SCE and an onset potential of 445±21 mV vs. SCE in air-equilibrated PBS (**Fig. 1D**).

The assembled EBFC registered a maximum current density (j_{max}) of 21.1 µA cm^{-2} at 77 mV, an open circuit voltage (OCV) of 0.471±0.02 V and a maximum power density (P_{max}) of 1.88±0.38 µW cm^{-2} at 0.122 V in air-equilibrated PBS solution containing 10 mM glucose (**Fig. 2A**). The obtained OCV (0.471 V) is essentially equivalent to the difference between the onset potentials of the bioanode (0 V) and biocathode (0.455 V). The substrate supply was considerably constrained by transport of O_2, as evidenced by the polarisation curve of the biocathode (**Fig. 1D**). In contrast, the same EBFC yielded a j_{max} of 17.7 µA cm^{-2} at 22 mV (*i.e.* a volumetric current density of 376.4 µA cm^{-3} based on the volume of the whole device comprising the PET-NPG based bioanode and biocathode and the PVA electrolyte), an OCV of 0.326±0.029 V and a P_{max} of 0.975±0.18 µW cm^{-2} (corresponding to a volumetric power density of 20.7±3.8 µW cm^{-3}) at 0.093 V when using PVA hydrogel as electrolyte. The decreased performance is likely a consequence of the limited mobility of glucose in the polymer matrix[10] and relatively low ionic conductivity (for comparison, the σ of 0.1 M pH 7.0 PBS at 25 °C is 11.6 mS cm^{-1}). The quasi-solid-state EBFC can be bent to an angle of up to 60° without significant changes in the output power density (**Fig. 2B, Fig. S1B**). This indicates that the NPG electrodes are mechanically robust and can withstand mechanical deformation without significant structural changes and film delamination[15]. The underlying Au protective layer ensured no considerable increase in sheet resistance[15]. This reasonably good flexibility enables attachment of the EBFC to the body. The flexible EBFC could be utilised to power wearable microelectronics irrespective of whether or not the subject is sweating.

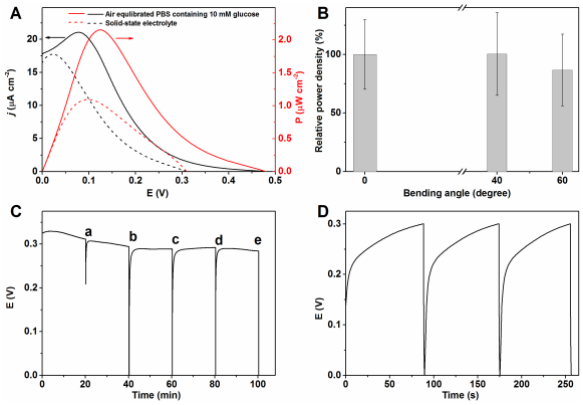

Fig. 2. (A) Power and polarisation curves for the EBFC obtained in aqueous solution (solid line) and using the solid-state hydrogel (dash line); (B) The relationship between bending angle of the flexible cell and relative power density; (C) Potential profile of the biocapacitor upon various discharging current densities; Experimental setup: reset at open-circuit (cutoff: 0.3 V), followed by discharging at 5 (a), 50 (b), 100 (c), 200 (d), 500 (e) μA cm^{-2} (cutoff: 0 V). (D) The initial three cycles of self-charge (cutoff: 0.3 V) and discharge of the biocapacitor with a discharge current density of 100 μA cm^{-2}.

The quasi-solid-state EBFC was tested as a self-powered biosupercapacitor. The capacitance of the device originated from the electrochemical double layer capacitance of the high-surface-area NPG and the pseudocapacitance of the osmium redox polymer[21, 22, 23, 30]. The assembled cell was reset at the open-circuit mode (cut-off at 0.3 V), followed by galvanostatic discharge at various current densities up to 500 μA cm^{-2} (cut-off at 0 V) (**Fig. 2C**). Interestingly, the potential of the built-in capacitor was discharged to zero, which can be restored towards the OCV of the EBFC in the subsequent reset step. In other words, the device was capable of generating repeat pulses. Discharging current densities of 500 and 200 μA cm^{-2} resulted in maximum instantaneous power densities of 70.5 and 34.9 μW cm^{-2}, respectively, 72 and 36 times greater than that delivered from an EBFC alone (0.975 μW cm^{-2}). The intrinsic nature of the supercapacitor permitted such significant improvement of instantaneous power density. Based on the galvanostatic discharge segment, the specific capacitance of the assembled cell was calculated to be 332±4 μF cm^{-2}, which is consistent with a previously reported value (357 μF cm^{-2}) of a NPG/Os polymer based biosupercapacitor[23]. The observed voltage drops during discharge indicated an ohmic resistance of 615±208 Ω. As a control, an assembled device consisting of Os polymer modified electrodes without enzymes displayed no potential-recovery behaviour after the first discharge.

The biosupercapacitor can be used for 620 cycles at a discharge current density of 100 μA cm^{-2} (**Fig. S3**). **Fig. 2D** shows the initial three cycles of self-charge and discharge. After discharging, the potential recovered to 0.3 V after 89 s. In the course of ca. 12-hour operation, the device exhibited a loss of 51.6% in maximum instantaneous power density (**Fig. 3**) with a half-life-time of ca. 11 h (at 610th cycle), demonstrating the cycling stability of the supercapacitor. The reset time to regain 0.3 V turned to be longer with long-term testing, which was 390 s for the 620th cycle. The decrease can be attributed to the inactivation of the BFC as result of enzyme deactivation and leaching of Os polymer[23]. This biosupercapacitor could potentially be used to load wound-healing drugs on skin, whose release can be electrically triggered by the EBFC generated stimuli, as demonstrated by Kai et al.[9]

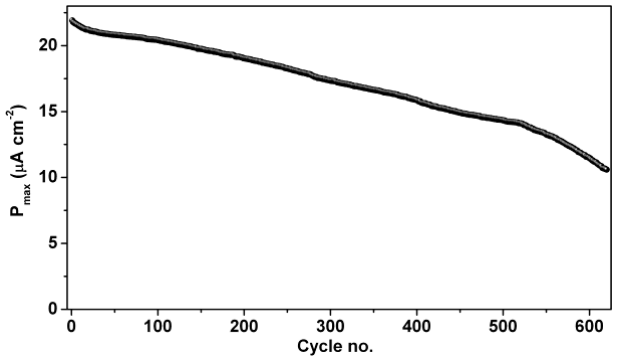

Fig. 3. Stability of the all-solid-state device for 620 cycles; Experimental protocol: reset at open-circuit for 20 min and cutoff at 0.3 V, followed by discharging at 0.1 mA cm^{-2} and cutoff at 0 V (**Fig. S3**).

In conclusion, a quasi-solid-state and flexible EBFC was prepared using enzyme modified NPG electrodes and PVA hydrogel film with preloaded sugar as the electrolyte. The self-powered biosupercapaictor showed considerable stability, which was able to deliver potential pulses for 620 cycles at 100 μA cm^{-2}, with maximum instantaneous power densities that are much higher than that observed with the EBFC alone. Based on the methodology of the current work, a skin-worn lactate/O_2 EFBC using hydrogel electrolyte stocking lactate can be developed, avoiding the constrain of the required sweat lactate. It could simultaneously

consume the lactate from sweat and hydrogel when the human subject is perspiring, while utilising the strode lactate when the human subject is in resting state.

Financial support from the European Commission (FP7-PEOPLE-2013-ITN “Bioenergy”) is acknowledged. X. Xiao acknowledges a Government of Ireland Postgraduate Scholarship (GOIPG/2014/659). We thank Prof. Dónal Leech and Dr. Peter Ó Conghaile for providing osmium redox polymers.

Notes and references

1 S. C. Barton, J. Gallaway and P. Atanassov, *Chem. Rev.*, 2004, **104**, 4867-4886.
2 K. MacVittie, J. Halamek, L. Halamkova, M. Southcott, W. D. Jemison, R. Lobel and E. Katz, *Energy Environ. Sci.*, 2013, **6**, 81-86.
3 M. Gamella, A. Koushanpour and E. Katz, *Bioelectrochem.*, 2018, **119**, 33-42.
4 A. J. Bandodkar, *J. Electrochem. Soc.*, 2017, **164**, H3007-H3014.
5 A. J. Bandodkar and J. Wang, *Electroanalysis*, 2016, **28**, 1188-1200.
6 W. Jia, G. Valdés-Ramírez, A. J. Bandodkar, J. R. Windmiller and J. Wang, *Angew. Chem. Int. Ed.*, 2013, **52**, 7233-7236.
7 I. Jeerapan, J. R. Sempionatto, A. Pavinatto, J.-M. You and J. Wang, *J. Mater. Chem. A*, 2016, **4**, 18342-18353.
8 Y. Ogawa, K. Kato, T. Miyake, K. Nagamine, T. Ofuji, S. Yoshino and M. Nishizawa, *Adv. Healthc. Mater.*, 2015, **4**, 506-510.
9 H. Kai, T. Yamauchi, Y. Ogawa, A. Tsubota, T. Magome, T. Miyake, K. Yamasaki and M. Nishizawa, *Adv. Healthc. Mater.*, 2017, **6**, 1700465.
10 M. Kizling, P. Biedul, D. Zabost, K. Stolarczyk and R. Bilewicz, *Electroanalysis*, 2016, **28**, 2444-2451.
11 T. Miyake, K. Haneda, S. Yoshino and M. Nishizawa, *Biosens. Bioelectron.*, 2013, **40**, 45-49.
12 Y. Ogawa, Y. Takai, Y. Kato, H. Kai, T. Miyake and M. Nishizawa, *Biosens. Bioelectron.*, 2015, **74**, 947-952.
13 M. Kaempgen, C. K. Chan, J. Ma, Y. Cui and G. Gruner, *Nano Lett.*, 2009, **9**, 1872-1876.
14 G. Wang, X. Lu, Y. Ling, T. Zhai, H. Wang, Y. Tong and Y. Li, *ACS Nano*, 2012, **6**, 10296-10302.
15 X. Xiao, T. Siepenkoetter, P. Ó. Conghaile, D. Leech and E. Magner, *ACS Appl. Mater. Interfaces*, 2018, **10**, 7107-7116.
16 X. Xiao and E. Magner, *Chem. Commun.*, 2015, **51**, 13478-13480.
17 U. Salaj-Kosla, M. D. Scanlon, T. Baumeister, K. Zahma, R. Ludwig, P. Ó. Conghaile, D. MacAodha, D. Leech and E. Magner, *Anal. Bioanal. Chem.*, 2013, **405**, 3823-3830.
18 C. Agnes, M. Holzinger, A. Le Goff, B. Reuillard, K. Elouarzaki, S. Tingry and S. Cosnier, *Energy Environ. Sci.*, 2014, **7**, 1884-1888.
19 D. Pankratov, Z. Blum, D. B. Suyatin, V. O. Popov and S. Shleev, *ChemElectroChem*, 2014, **1**, 343-346.
20 M. Kizling, S. Draminska, K. Stolarczyk, P. Tammela, Z. Wang, L. Nyholm and R. Bilewicz, *Bioelectrochem.*, 2015, **106, Part A**, 34-40.
21 D. Pankratov, F. Conzuelo, P. Pinyou, S. Alsaoub, W. Schuhmann and S. Shleev, *Angew. Chem. Int. Ed.*, 2016, **55**, 15434-15438.
22 K. L. Knoche, D. P. Hickey, R. D. Milton, C. L. Curchoe and S. D. Minteer, *ACS Energy Lett.*, 2016, 380-385.
23 X. Xiao, P. Ó. Conghaile, D. Leech, R. Ludwig and E. Magner, *Biosens. Bioelectron.*, 2017, **90**, 96-102.
24 T. Bobrowski, E. González Arribas, R. Ludwig, M. D. Toscano, S. Shleev and W. Schuhmann, *Biosens. Bioelectron.*, 2018, **101**, 84-89.
25 S. Shleev, E. González-Arribas and M. Falk, *Curr. Opin. Electrochem.*, 2017, **5**, 226-233.
26 C. Hou and A. Liu, *Electrochim. Acta*, 2017, **245**, 303-308.
27 H. S. Mansur, R. L. Oréfice and A. A. P. Mansur, *Polymer*, 2004, **45**, 7193-7202.
28 S. Petty-Weeks, J. J. Zupancic and J. R. Swedo, *Solid State Ion.*, 1988, **31**, 117-125.
29 U. Salaj-Kosla, S. Pöller, Y. Beyl, M. D. Scanlon, S. Beloshapkin, S. Shleev, W. Schuhmann and E. Magner, *Electrochem. Commun.*, 2012, **16**, 92-95.
30 X. Xiao, P. Ó. Conghaile, D. Leech, R. Ludwig and E. Magner, *Biosens. Bioelectron.*, 2017, **98**, 421-427.